over 200 with signal dynamic ranges of ~225, which are much lower than the potentially maximum ranges, and which were partly limited by the high background levels caused by the laser. As can be expected, the penetration distance increases with the jet-to-freestream velocity ratio. The spreading of the jet is also seen to increase as the velocity ratio increases toward 20:1, where the jet flame length as defined by Broadwell and Breidenthal[6] should be a minimum.[7] The most interesting features in all of these images are, however, the "fingers" that separate from the jet and travel toward the wall in the wake region. The jet fluid concentration of these structures is quite low, and in some cases they might be buried in the background noise of a poor detection system. If the images are displayed with a linear gray scale, nothing between the jet and the tunnel wall can be discerned (see Fig. 3).

The instantaneous images have been compared to an average jet centerline trajectory calculated with the expression (see Pratte and Baines[8])

$$\frac{y}{rd_0} = 2.05*\left(\frac{x}{rd_0}\right)^{0.28}$$

where r is the jet-to-crossflow ratio and d_0 is the source diameter, for r ranging from 5 to 35. Figure 3 displays an instantaneous image (with $r = 11.5$) on which the calculated jet centerline location, obtained with the preceding formula, is superposed. The same excellent agreement between calculated and measured jet positions has been observed for the other r values studied.

Although eddies of crossflow fluid penetrating the jet have been previously observed,[9,10] the opposite case, which is found in our images (jet fluid entering the wake), has to our knowledge never been reported. Furthermore, the absence of this jet/crossflow interaction was interpreted by Fric and Roshko[9] as evidence that the jet vorticity does not contribute to the wake vorticity. It is possible, however, that they were not able to detect these structures due to a lack of sensitivity in their experiments (smoke-wire visualization). It is also possible that some jet fluid may flow axially into the cores of the wake vortices once they have formed.[11] In any event, more images are required to formulate any statement about these wake detachments; e.g., what are the conditions determining their presence, their possible dependence on velocity ratio or jet Reynolds number, orientation with respect to the jet and wall, etc.

In Fig. 4, the same image shown in Fig. 3 (right) is displayed as a rendered surface where intensities have been mapped into heights. Prior to the rendering, a 3×3 smoothing filter was applied to the original image to decrease noise fluctuations. This type of presentation facilitates the visual analysis of gradient magnitudes and quantitative distribution of fluid concentration. This jet centerline concentration decay is easily observed, together with the existence of areas of nearly uniform concentration. The complexity of smaller scale details is also evidenced, whereas the wake region is more readily discernible.

The results presented here provide confirmation of the utility of PLIF imaging of acetone for fundamental studies in fluid mechanics, and also suggest the need for a more detailed investigation that could lead to deeper understanding of scalar mixing in transverse jets. Because the interesting features involve low concentrations, it is essential to use high-sensitivity detectors. A thin, backside-illuminated CCD array can be considered the "state of the art" device for this type of measurement, especially when imaging acetone fluorescence. To maximize the emitted signal, however, high energy excitation lasers should still be used.

Acknowledgments

This work has been sponsored by the Air Force Office of Scientific Research, Aerospace Sciences Directorate, with Julian Tishkoff as the technical monitor. S. H. Smith is supported by the NDSEG fellowship.

References

[1]Dimotakis, P. E., Miake-Lye, R. C., and Papantoniou, D. A., "Structure and Dynamics of Round Turbulent Jets," *Physics of Fluids*, Vol. 26, No. 11, 1983, pp. 3185–3192.

[2]Hanson, R. K., Seitzman, J. M., and Paul, P. H., "Planar Laser-Induced Fluorescence Imaging of Combustion Gases," *Applied Physics B*, Vol. 50, No. 6, 1990, pp. 441–454.

[3]van Cruyningen, I., Lozano, A., and Hanson, R. K., "Quantitative Imaging of Concentration by Planar Laser Induced Fluorescence," *Experiments in Fluids*, Vol. 10, No. 1, 1990, pp. 41–49.

[4]Lozano, A., Yip, B., and Hanson, R. K., "Acetone: a Tracer for Concentration Measurements in Gaseous Flows by Planar Laser-Induced Fluorescence," *Experiments in Fluids*, Vol. 13, 1992, pp. 369–376.

[5]Lozano, A., "Laser- Excited Luminescent Tracers for Planar Concentration Measurements in Gaseous Jets," High Temperature Gas Dynamics Lab. Rept. T-284, Stanford Univ., Stanford, CA, 1992.

[6]Broadwell, J. E., and Breidenthal, R. E., "Structure and Mixing of a Transverse Jet in Incompressible Flow," *Journal of Fluid Mechanics*, Vol. 148, Nov. 1984, pp. 405–412.

[7]Karagozian, A. R., "The Flame Structure and Vorticity Generated by a Chemically Reacting Transverse Jet," *AIAA Journal*, Vol. 24, No. 9, 1986, pp. 1502–1507.

[8]Pratte, B. D., and Baines, W. D., "Profiles of the Round Turbulent Jet in a Cross Flow," *Journal of the Hydronautical Division of the American Society of Civil Engineers*, Vol. 92, Nov. 1967, pp. 53–64.

[9]Fric, T. F., and Roshko, A., "Structure in the Near Field of the Transverse Jet," 7th Symposium on Turbulent Shear Flows, Paper 6-4, Stanford, CA, Aug. 1989.

[10]Fric, T. F., "Structure in the Near Field of the Transverse Jet," Ph.D. Thesis, California Inst. of Technology, Pasadena, CA, 1990.

[11]Roshko, A., private communication, California Inst. of Technology, Pasadena, CA, 1993.

Effects of In-Plane Displacements on Frequency and Damping of Composite Laminates

Kyo-Nam Koo* and In Lee†
Korea Advanced Institute of Science and Technology, Taejon 305-701, Republic of Korea

Introduction

TRANSVERSE shear deformation plays an important role in anisotropic plates since most of the advanced composites have a low ratio of the transverse shear modulus to the modulus in the fiber direction. Although the shear deformation plate theory is adequate for predicting the global responses of medium-thick laminated plates such as deflection, natural frequency, and buckling load, it fails to give accurate predictions for transverse shear stresses and in-plane displacements. The fact that the damping characteristics are affected by the local behavior of plate deformation whereas the natural frequency is determined by global deformation requires a refined theory for the damping analysis of composite laminated plates.

The various approaches used for modeling multilayered composite plates were reviewed by Noor and Burton.[1] The fundamental frequency and the associated mode shape of free-vibration problems were considered in several papers.[2,3] However, the effect of the in-plane displacements on the damping characteristics of composite laminates has not been studied in the previous papers. Research on the damping analysis of composite plates is not so extensive as that on the undamped free-vibration analysis. Lin et al.[4] used a damped element model to evaluate the specific damping capacity (SDC) of composite plates. In spite of the great contribution their work made to this field of study, the effect of the

Received Jan. 14, 1993; revision received May 28, 1993; accepted for publication May 30, 1993.

*Graduate Research Assistant, Department of Aerospace Engineering, 373-1, Kusong-dong, Yusong-gu.

†Associate Professor, Department of Aerospace Engineering, 373-1, Kusong-dong, Yusong-gu. Member AIAA.

in-plane displacement variation through the thickness on damping was not been investigated in their work.

In this paper, the effects of the in-plane displacements on the frequency and damping characteristics are investigated for the cross-ply laminated plates in cylindrical bending vibration. The cylindrical bending problem makes the physical interpretation clear without confronting the additional complexities of fully three-dimensional behavior.

Analysis

Consider a cross-ply laminate composed of n layers in cylindrical bending as shown in Fig. 1. Because the solution is independent of y and there is no displacement in the y direction, the displacement field should be expressed of the form

$$\begin{aligned} u(x, z, t) &= u_0(x, t) + U(x, z, t) \\ w(x, z, t) &= w_0(x, t) \end{aligned} \tag{1}$$

where u_0 and w_0 are the displacements in the middle plane in x and z directions, respectively, and $U(x, 0, t) = 0$. In Eq. (1), the transverse normal strain is neglected, which is particularly true for the vibrational response.[1] Based on the generalized laminated plate theory (GLPT),[5] U is approximated across the coordinate z as

$$U(x, z, t) = \sum_{J=1}^{N} U_J(x, t)\Phi^J(z) \tag{2}$$

where N is the number of degrees of freedom along the thickness and Φ^J is the Lagrangian interpolation function.

Finite element formulation using Eqs. (1) and (2) gives the equation of motion in the form of a standard eigenvalue problem for free-vibrational analysis:

$$(\boldsymbol{K} - \omega^2 \boldsymbol{M})\boldsymbol{u} = 0 \tag{3}$$

where $\boldsymbol{K}$ and $\boldsymbol{M}$ are the stiffness and mass matrices, respectively.

The dissipated energy of the composite laminate in cylindrical bending vibration is composed of two components:

$$\Delta E = \frac{1}{2}\int_0^l \int_{-h/2}^{h/2} (\psi_x \sigma_x \epsilon_x + \psi_{xz}\tau_{xz}\gamma_{xz})\,\mathrm{d}z\,\mathrm{d}x = \frac{1}{2}\boldsymbol{u}^T\boldsymbol{K}_d\boldsymbol{u} \tag{4}$$

where E is the maximum strain energy, ψ_x and ψ_{xz} are the specific damping capacities (SDC) related to their stress components, and $\boldsymbol{K}_d$ is referred to as the damped stiffness matrix. Then, the SDC for each mode is computed as follows[4]:

$$\Psi_i = \frac{\Delta E}{E} = \frac{\phi_i^T K_d \phi_i}{\phi_i^T K \phi_i} \tag{5}$$

where ϕ_i is the ith modal vector obtained from the eigenanalysis of Eq. (3).

Results and Discussions

In this paper, the material properties of a fiber-reinforced composite are used:

$$E_1/E_2 = 25, \qquad G_{12}/E_2 = G_{13}/E_2 = 0.5, \qquad G_{23}/E_2 = 0.2$$

$$\nu_{12} = 0.25, \qquad \psi_1 = 0.0045, \qquad \psi_2 = 0.0422$$

$$\psi_{12} = \psi_{13} = \psi_{23} = 0.0705$$

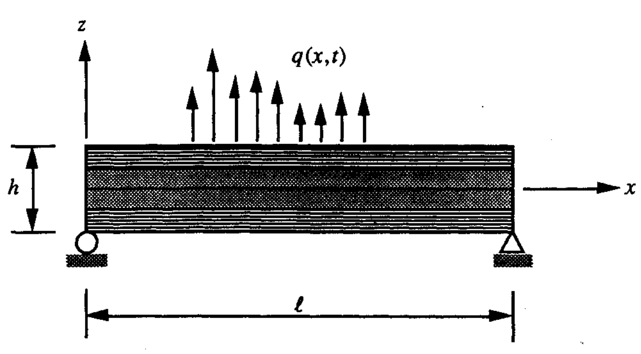

Fig. 1 Coordinate system of laminated plate in cylindrical bending.

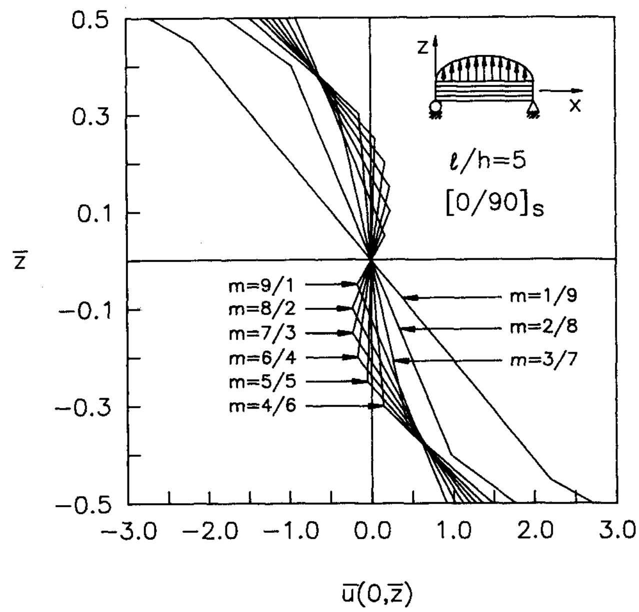

Fig. 2 Variation of in-plane displacements for simply supported [0/90]$_S$ plate with cross-ply ratios: l/h = 5.

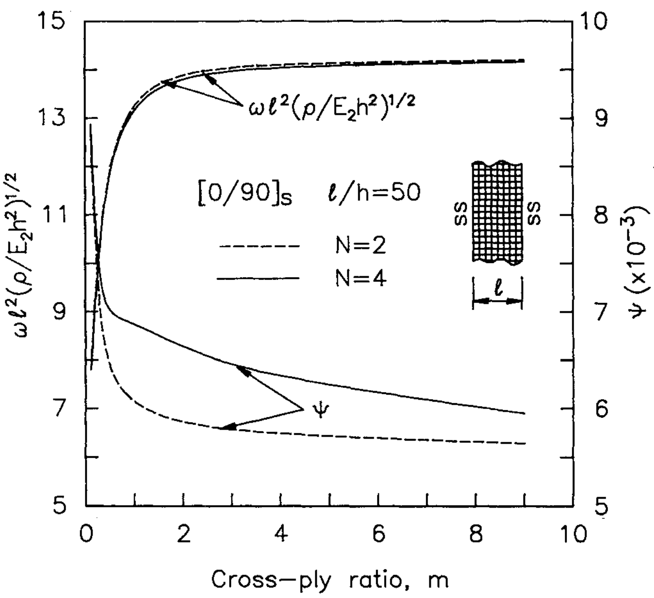

Fig. 3 Effects of cross-ply ratio on fundamental frequencies and SDC for [0/90]$_S$ thin plates: l/h = 50.

The following normalized variables are used in presenting results:

$$\bar{u} = \frac{uE_2h^2 \times 100}{q_0 l^3}, \qquad \bar{\omega} = \omega l^2 \sqrt{\frac{\rho E_2}{h^2}}, \qquad \bar{z} = \frac{z}{h} \tag{6}$$

The variation of the in-plane displacements $\bar{u}(0, \bar{z})$ for various cross-ply ratios m are shown in Fig. 2 when simply supported [0/90]$_S$ plates are subjected to the sinusoidal loading, $q_0\sin(\pi x/l)$. The length-to-thickness l/h ratio, is 5 in this case. The thickness of the cross-ply laminates is the same for the various cross-ply ratios m which is defined as the ratio of total thickness of 0-deg layers to total thickness of 90-deg layers. The results in Fig. 2 imply that the variation of the in-plane displacements through the thickness can have a great

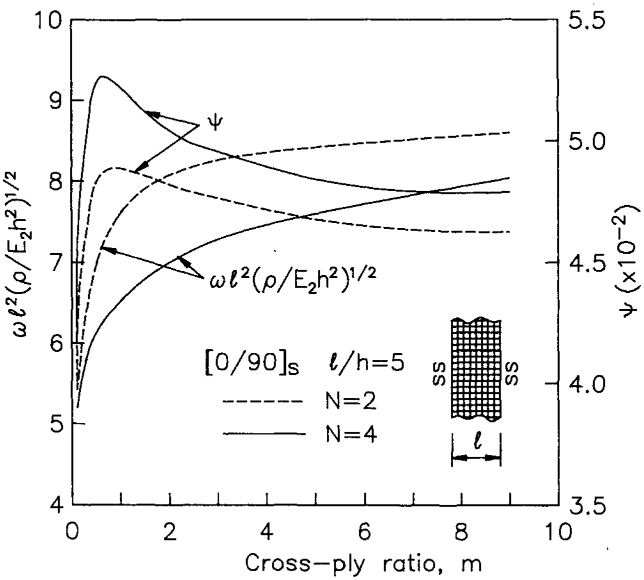

Fig. 4 Effects of cross-ply ratio on fundamental frequencies and SDC for $[0/90]_S$ thick plates: $l/h = 5$.

influence on the local behavior such as the damping characteristics of composite laminates.

Figure 3 shows the fundamental frequencies and the SDC for a simply supported thin plate with $l/h = 50$. The results for $N = 4$ are obtained by dividing the laminate through the thickness into four sections. Those for $N = 2$, which are close to solutions of the first-order shear deformation theory in the case of symmetric laminates, are obtained by dividing the laminate into two sections. The results for $N = 4$ are more accurate than those for $N = 2$. There is a little difference between the fundamental frequencies for $N = 4$ and $N = 2$ in this thin plate. However, the SDC for $N = 2$ are estimated to be smaller than those for $N = 4$. This is due mainly to the underestimation of the transverse shear deformation for $N = 2$ by neglecting the variation of the in-plane displacements through the thickness. The transverse shear deformation is small for this thin plate and the damping characteristics of the laminate in bending are severely dependent on the amount of 90-deg layer. Hence, as m increases, the SDC decreases.

The results for a thick $[0/90]_S$ plate with $l/h = 5$ are shown in Fig. 4. These results for the thick plate are different from those for the thin plate with $l/h = 50$. In this thick plate, there is considerable error in the frequencies and the SDC for $N = 2$. The SDC is at the highest value near $m = 4/6$ since the transverse shear deformation is the largest at $m = 4/6$. Therefore, it is concluded from this fact that the SDC for a thick laminate is greatly dependent on the degree of the transverse shear. The multilayered theory which can accurately describe the in-plane displacement variation through the thickness is required for the accurate estimation of the SDC.

Conclusions

To investigate the effects of the layer-wise in-plane displacements on the vibration and damping characteristics of composite laminates, the finite element method has been formulated based on the layer-wise distribution of the in-plane displacements. The SDC of each mode was obtained by the modal strain energy method. The numerical results show that variation of in-plane displacements through the thickness does not have much influence on the natural frequency, but has a great influence on the damping of composite plates, especially on the damping of thick composite plates, because the damping is affected by local behavior whereas the natural frequency is affected by global behavior. Also, the cross-ply ratio of composite laminate affects the vibration and damping characteristics because it determines the deformation pattern such as bending and transverse shear deformation. The thick plate has the highest damping near the cross-ply ratio of 1.0. For the thin plate, the smaller the cross-ply ratio becomes, the higher the SDC becomes.

References

[1]Noor, A. K., and Burton, W. S., "Assessment of Shear Deformation Theories for Multilayered Composite Plates," *Applied Mechanics Reviews,* Vol. 41, No. 1, 1989, pp. 1–13.

[2]Reddy, J. N., and Kuppusamy, T., "Natural Vibrations of Laminated Anisotropic Plates," *Journal of Sound and Vibration,* Vol. 94, No. 1, 1984, pp. 63–69.

[3]Owen, D. R. J., and Li, Z. H., "A Refined Analysis of Laminated Plates by Finite Element Displacement Methods—II. Vibration and Stability," *Computers and Structures,* Vol. 26, No. 6, 1987, pp. 915–923.

[4]Lin, D. X., Ni, R. G., and Adams, R. D., "Prediction and Measurement of the Vibration Damping Parameters of Carbon Glass Fiber-Reinforced Plastics Plates," *Journal of Composite Materials,* Vol. 18, March 1984, pp. 132–152.

[5]Reddy, J. N., Barbero, E. J., and Teply, J. L., "A Plate Bending Element Based on a Generalized Laminated Plate Theory," *International Journal for Numerical Methods in Engineering,* Vol. 28, No. 10, 1989, pp. 2275–2292.